Proceedings of IDETC/CIE 2005
ASME 2005 International Design Engineering Technical Conferences
& Computers and Information in Engineering Conference
September 24-28, 2005, Long Beach, California USA

DETC2005-84671

STABILITY-OPTIMIZED CLEARANCE CONFIGURATION OF FLUID-FILM JOURNAL BEARINGS

Koichi Matsuda
Kyushu University
6-10-1 Hakozaki,
Fukuoka, 812-8581, JAPAN
matsuda@mech.kyushu-u.ac.jp

Yoichi Kanemitsu
Kyushu University
6-10-1 Hakozaki,
Fukuoka, 812-8581, JAPAN
kanemitu@mech.kyushu-u.ac.jp

Shinya Kijimoto
Kyushu University
6-10-1 Hakozaki,
Fukuoka, 812-8581, JAPAN
kiji@mech.kyushu-u.ac.jp

ABSTRACT

A clearance configuration of fluid-film journal bearings is optimized in a sense of enhancing the stability of a full circular bearing at high rotational speeds. A performance index is chosen as the sum of the squared whirl-frequency ratios over a wide range of eccentricity ratios, and a Fourier series is used to represent an arbitrary configuration of fluid-film bearings. An optimization problem is then formulated to find the Fourier coefficients to minimize the index. The whirl-frequency ratio is inversely proportional to the stability threshold speeds of a Jeffcott rotor. The short bearing approximation is used to simplify a mathematical model that describes a pressure distribution developed in a fluid-film bearing. The designed bearing cannot destabilize the Jeffcott rotor at any high rotating speed subject to the short-bearing assumption and significantly reduces the size of the unstable region for a finite-length bearing with a small length-to-diameter ratio.

INTRODUCTION

Fluid-film journal bearings are widely used to support a rotating machinery system, and those bearings often have a clearance configuration of a full circle. However, it is well known that the full circular bearings destabilize the system at high rotational speeds, which is called the whirl instability. The whirl instability occurs due to the presence of skew-symmetric stiffness coefficients. Many types of clearance configuration have been suggested in place of a full circle to solve this instability problem [1]. Although the stability problem is certainly improved by them, there still exist any other configuration that has stability characteristics better than those configurations. By the way, many clearance optimization problems have been solved to increase the static load capacity of fluid-film journal bearings [2-8]. Hashimoto [9] also found an optimal clearance configuration that minimizes the weighted sum of fluid-film temperature rise and supply lubricant quantity. A stability-related optimization problem was also solved for a fluid-film journal bearing in recent years. Wang et al. [10] designs an elliptical bearing with high eccentricity ratio and two large pressure zones for high-speed stability by maximizing film pressures in the upper and lower lobes. The current authors [11-13] found an optimal clearance configuration that minimizes the sum of the attitude angles over a region of eccentricity ratio. This optimization criterion aims to eliminate the cross-coupling terms of the stiffness coefficients for enhancing the stability of a fluid-film journal bearing. The designed bearings originally had load capacity when the journal is situated at the bearing center [11, 12] and are modified to have a rotationally symmetric clearance configuration without load capacity at the situation of the journal [13]. The designed bearings successfully increase the stability threshold speeds of a simple rotating-machinery system, and, however, the attitude angles are not necessarily small for a fluid-film bearing with good stability characteristics. Recently, Swanson [14] obtained an optimal clearance configuration that minimizes the maximum value of the whirl-frequency ratios in a wide range of bearing loads at a specific rotating speed. The whirl-frequency ratios are inversely proportional to the stability threshold speed of a Jeffcott rotor with a very flexible shaft and depend only on the stiffness and damping coefficients of a fluid-film bearing [1]. The stability of the designed bearings is significantly improved compared with those of the previously designed bearings with a fixed configuration, and the Jeffcott-rotor system is stable at any frequency for all the bearing loads at the specific rotating speed. However, the optimization problem is formulated using the specific values of the bearing length and diameter, rotating speed, and bearing loads, and the results are less general in this sense.

This paper treats another optimization problem for a clearance configuration of fluid-film journal bearings. This optimization aims to enhance stability characteristics of a full circular bearing. The performance index is chosen as the sum of the whirl-frequency ratios over a wide range of eccentricity ratios. The performance index is more closely related to stability of a rotating machinery system than that of the previous work of the authors, the attitude angles. However, the

whirl-frequency ratio is a function of stiffness and damping coefficients of a fluid-film bearing, and it significantly increases computational time to solve the optimization problem. The short bearing model is thus used to reduce the computational time because the model gives an analytical solution to the Reynolds equation that describes a pressure distribution developed in a fluid-film bearing. Moreover, it is assumed that the circumferential clearance configuration is only optimized and that the configuration is constant in the axial direction. This clearance optimization is thus expected to be effective only in the case that bearing length is shorter than bearing diameter. Therefore, it does not matter that the short-bearing model is limited to the case that bearing length is infinitely short. A Fourier series is used with a period of π [rad] to represent an arbitrary clearance configuration of fluid-film bearings. The designed bearings have no load capacity owing to the periodicity when the journal is situated at the bearing center. An optimization problem is then formulated to find the Fourier coefficients to minimize the performance index. The optimization problem is numerically solved, and it is shown that the designed bearing cannot destabilize the Jeffcott rotor at any high rotating speed subject to the short-bearing assumption. This assumption does not hold for many fluid-film bearings with finite length, and the stability threshold speeds of a Jeffcott rotor are computed by a finite difference method for finite-length bearings that have the designed clearance configuration. It is shown that the designed bearing significantly reduces the size of the unstable region for L/D =0.1. The Reynolds equation is solved without specific values of the variables, and the optimization results are more general in this sense than those of Swanson [14].

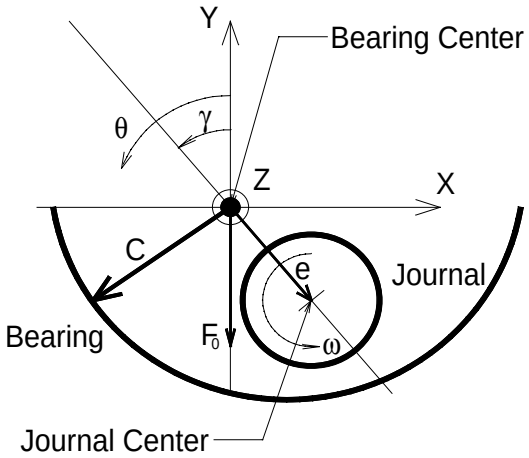

Fig.1 Configuration of a fluid-film journal bearing

MATHEMATICAL MODEL OF FLUID-FILM JOURNAL BEARING

A pressure distribution developed in a fluid-film journal bearing is well described by the Reynolds equation, and the closed-form solution to the equation can be obtained in the case that the bearing length is sufficiently shorter than the bearing diameter. The Reynolds equation for a constant-viscosity incompressible fluid can be written in polar-cylindrical coordinates (Fig.1) as

$$R^{-2}\frac{\partial}{\partial\theta}\left(\frac{H^3}{12\mu}\frac{\partial p}{\partial\theta}\right)+\frac{\partial}{\partial z}\left(\frac{H^3}{12\mu}\frac{\partial p}{\partial z}\right)=-\frac{U_2}{2R}\frac{\partial H}{\partial\theta}+V_2 \qquad (1)$$

where R is bearing radius, H film thickness, μ viscosity, and p pressure in a fluid film of a journal bearing. Moreover, U_2 and V_2 are the velocity components at the journal surface. In this study, the boundary conditions enforced on the pressure solution are
For the axial direction:

$$p(\theta,\pm L/2)=0 \quad \text{and} \quad \partial p/\partial z(\theta,0)=0 \qquad (2)$$

For the circumferential direction:

$$p(\theta,z)=p(\theta+2\pi,z) \qquad (3)$$

Equation (1) is rewritten in a dimensionless form to give

$$\frac{\partial}{\partial\theta}\left(h^3\frac{\partial\overline{p}}{\partial\theta}\right)+\frac{\partial}{\partial\hat{z}}\left(h^3\frac{\partial\overline{p}}{\partial\hat{z}}\right)=-\frac{\overline{U}_2}{2}\frac{\partial h}{\partial\theta}+\overline{V}_2\equiv g \qquad (4)$$

where $H=C_r h$, $p=\overline{p}(12\mu\omega R^2/C_r^2)$, $U_2=R\omega\overline{U}_2$, $V_2=C_r\omega\overline{V}_2$, $z=R\hat{z}$, and C_r denotes the minimum clearance of the bearing. It is assumed that the clearance ratio, C_r/R , is sufficiently smaller than unity. The right hand side of Eq. (4) is then rewritten as

$$g(\theta)=-\frac{1}{2}\frac{\partial h}{\partial\theta}+\tilde{x}\cos\theta+\tilde{y}\sin\theta+\tilde{x}'\sin\theta-\tilde{y}'\cos\theta \qquad (5)$$

where γ is the attitude angle, $\tilde{x}=\varepsilon\sin\gamma$, $\tilde{y}=-\varepsilon\cos\gamma$, and the prime denotes the differentiation with respect to dimensionless time $\bar{t}=\omega t$. For the details of Eq. (5), see Child [1]. The short bearing model is used to obtain the closed-form solution to Eq. (4). That is, it is assumed that the bearing length is sufficiently short compared with the bearing diameter. The first term is then neglected on the left hand side of Eq. (4) to give

$$\frac{\partial}{\partial\hat{z}}\left(h^3\frac{\partial\overline{p}}{\partial\hat{z}}\right)=g \qquad (6)$$

Equation (6) is analytically integrated with respect to $\hat{z}$, and the integration constants are uniquely determined to satisfy the boundary condition Eq. (2) to yield

$$\overline{p}(\theta,\hat{z})=\frac{g}{2h^3}\left(\hat{z}^2-\tau^2\right) \qquad (7)$$

where $\tau=L/D$ with bearing diameter $D=2R$, and $-\tau\le\hat{z}\le\tau$. The pressure solution of Eq. (7) is still dependent of the axial coordinate $\hat{z}$. To eliminate the dependency on $\hat{z}$,

Eq. (7) is axially integrated to yield an average value of the pressure in the axial direction

$$\frac{1}{L}\int_{-L/2}^{L/2}\bar{p}(\theta,z)dz=\frac{1}{2\tau}\int_{-\tau}^{\tau}\bar{p}(\theta,\hat{z})d\hat{z}=-\frac{\tau^2 g}{3h^3}\equiv\frac{\tau^2\tilde{p}(\theta)}{3} \quad (8)$$

where

$$\tilde{p}(\theta)\equiv-\frac{g}{h^3}=\frac{3}{2\tau^3}\int_{-\tau}^{\tau}\bar{p}(\theta,\hat{z})d\hat{z} \quad (9)$$

Here, pressure $\tilde{p}$ is independent of the length-to-diameter ratio of the bearing, whereas the conventional short-bearing solution, Eq. (8), is not. The reaction force of the fluid-film is computed by integrating the pressure over the journal surface. It is assumed that only the positive values of the pressure contributes to integrating the reaction force of the fluid-film, that is, the pressure solution should satisfy the Gümbel boundary condition. When the rotor-bearing system is in a steady state, the reaction force is mathematically expressed as follows:

$$F_0=\sqrt{F_{x0}^2+F_{y0}^2} \quad (10)$$

with

$$F_{x0}\equiv\int_{p_0>0}p_0\sin\theta d\theta dz \quad \text{and} \quad F_{y0}\equiv-\int_{p_0>0}p_0\cos\theta d\theta dz \quad (11)$$

where the subscript 0 denotes the steady state, and F_{x0} and F_{y0} are x - and y -components of the reaction force F_0, respectively. For later convenience, the reaction force is rewritten in a dimensionless form to give

$$F_0=\tilde{F}_0(16\mu\omega\tau^3R^4/C_r^2) \quad (12)$$

where

$$\tilde{F}_0=\sqrt{\tilde{F}_{x0}^2+\tilde{F}_{y0}^2} \quad \text{with} \quad \tilde{F}_{x0}\equiv\int_\Theta\tilde{p}_0\sin\theta d\theta \quad \text{and}$$
$$\tilde{F}_{y0}\equiv-\int_\Theta\tilde{p}_0\cos\theta d\theta, \quad (13)$$

and pressure p_0 takes a positive value for $\theta\in\Theta$ with Θ independent of $\hat{z}$. By the way, stiffness and damping coefficients are computed by integrating pressure derivatives with respect to displacement and velocity of the journal center. The dimensionless stiffness and damping coefficients are related to the dimensional ones as follows:

$$k_{ij}=(C_r/F_0)K_{ij} \quad \text{and} \quad c_{ij}=(C_r\omega/F_0)C_{ij} \quad (14)$$

Moreover, Eq. (14) is rewritten by Eqs. (12) and (13) as follows:

$$k_{xx}=-\tilde{F}_0^{-1}\left(\partial\tilde{F}_x/\partial\tilde{x}\right)_0,\quad k_{xy}=-\tilde{F}_0^{-1}\left(\partial\tilde{F}_x/\partial\tilde{y}\right)_0,$$
$$k_{yx}=-\tilde{F}_0^{-1}\left(\partial\tilde{F}_y/\partial\tilde{x}\right)_0,\quad k_{yy}=-\tilde{F}_0^{-1}\left(\partial\tilde{F}_y/\partial\tilde{y}\right)_0,$$

$$c_{xx}=-\tilde{F}_0^{-1}\left(\partial\tilde{F}_x/\partial\tilde{x}'\right)_0,\quad c_{xy}=-\tilde{F}_0^{-1}\left(\partial\tilde{F}_x/\partial\tilde{y}'\right)_0,$$
$$c_{yx}=-\tilde{F}_0^{-1}\left(\partial\tilde{F}_y/\partial\tilde{x}'\right)_0,\quad c_{yy}=-\tilde{F}_0^{-1}\left(\partial\tilde{F}_y/\partial\tilde{y}'\right)_0, \quad (15)$$

where the derivations of the reaction force to the journal displacement and the journal velocity are given by integrating the pressure derivatives, for an example,

$$\left(\partial\tilde{F}_x/\partial\tilde{x}\right)_0=\int_\Theta\left(\partial\tilde{p}/\partial\tilde{x}\right)\big|_0\sin\theta d\theta \quad (16)$$

It is noted that integration region Θ generally varies the size depending on the journal displacement and velocity but the dependency does not affect the values of the bearing coefficients because the pressure always takes a value of zero at the boundary of Θ in the present study. Moreover, clearance magnitude is sufficiently smaller than a bearing diameter, and dimensionless film-thickness is given by

$$h(\varepsilon,\theta)=c(\theta)+\varepsilon\cos(\theta-\gamma)=c(\theta)-\tilde{y}\cos\theta+\tilde{x}\sin\theta \quad (17)$$

where $c=C/C_r$ with C being a clearance configuration of a fluid-film journal bearing. The pressure derivatives are used for computing the bearing coefficients and given by differentiating Eq. (13). Moreover, Eq. (23) is differentiated by

$$\frac{\partial h}{\partial\tilde{x}}=\sin\theta,\quad \frac{\partial h}{\partial\tilde{y}}=-\cos\theta,\quad \frac{\partial g}{\partial\tilde{x}}=\frac{1}{2}\cos\theta,$$
$$\frac{\partial g}{\partial\tilde{y}}=\frac{1}{2}\sin\theta,\quad \frac{\partial g}{\partial\tilde{x}'}=\sin\theta,\quad \frac{\partial g}{\partial\tilde{y}'}=-\cos\theta \quad (18)$$

To compare stability characteristics for different configuration of fluid-film bearings, the Sommerfeld number is introduced and defined by

$$S=\mu\left(\frac{\omega}{2\pi}\right)\left(\frac{R}{C_r}\right)^2\frac{DL}{F_0}=\frac{\tau}{12\pi\bar{F}_0} \quad (19)$$

where $F_0=\left(24\mu\omega R^4/C_r^2\right)\bar{F}_0$. To investigate static properties of the designed bearing, the friction coefficient of fluid-film bearings is defined as a dimensionless friction torque applied on the bearing surface:

$$\varsigma=(R/C_r)F_J/F_0 \quad (20)$$

where friction torque F_J is given by integrating the shear force on the bearing surface

$$F_J=\iint\mu\frac{\partial u}{\partial y}\bigg|_{y=h}Rd\theta dz \quad (21)$$

FORMULATION OF OPTIMIZATION PROBLEM

An optimization problem is formulated uniquely to determine the clearance configuration of the journal bearings. A

Optimization Problem

For given values of α, $h_{\min}$, δ, and $\bar{\varepsilon}_j$'s, find $\Pi = \left[X^T \quad \Gamma^T \quad d_1 \quad d_2 \quad q\right]^T$ to minimize the performance index:

$$J = \sum_{k=1}^{M} Max\left[\Omega_s^2(\bar{\varepsilon}_k), 0\right]$$
$$\left(0 < \bar{\varepsilon}_1 < \bar{\varepsilon}_2 < \cdots < \bar{\varepsilon}_M \equiv 1-\alpha < 1\right)$$

subject to the constraints:

$$\psi_k(\gamma_k, X) \equiv \tan\gamma_k + \left(\int_\Theta \tilde{p}_0(\bar{\varepsilon}_k)\sin(\theta-\gamma_k)d\theta \Big/ \int_\Theta \tilde{p}_0(\bar{\varepsilon}_k)\cos(\theta-\gamma_k)d\theta\right) = 0 \quad (k = 1,2,\cdots,M)$$

$$\psi_{M+1}(X, d_1) = X^T X + d_1^2 - \alpha^2 = 0$$

$$\psi_{M+2}(X, \gamma_M, q) = \frac{\partial \bar{h}}{\partial\theta}(\bar{\varepsilon}_M, \theta_{\min}) = 0$$

$$\psi_{M+3}(X, \gamma_M, q, d_2) = \bar{h}(\bar{\varepsilon}_M, \theta_{\min}) - h_{\min} - d_2^2 = 0$$

where

$X = \left[X_1 \quad X_2 \quad \cdots \quad X_{2K}\right]^T$, $\Gamma = [\gamma_1 \quad \gamma_2 \quad \cdots \quad \gamma_M]^T$, and $\theta_{\min} = \pi + \gamma_M + \delta\sin q$

Fig. 2 Optimization problem for clearance configuration of fluid-film journal bearings

Fourier series is here used to represent an arbitrary clearance configuration as follows:

$$C = \bar{C}\left\{1 + \sum_{k=1}^{K}\left[X_{2k-1}\cos 2k\theta + X_{2k}\sin 2k\theta\right]\right\} \qquad (22)$$

where $\bar{C}$ is now the mean value of the clearance over the entire clearance $\theta \in [0, 2\pi]$ and K the order of the series. Equation (22) means that the clearance is circumferentially a continuous and smooth function of θ and constant in the axial direction. Furthermore, the clearance configuration has a period of π [rad], and, therefore, the designed bearings have no load carrying capacity when the journal is situated at the bearing center, that is, $\varepsilon = 0$. For the later convenience, the fluid-film thickness of Eq. (17) is rewritten as

$$\bar{h}(\bar{\varepsilon}, \theta) = 1 + \bar{\varepsilon}\cos(\theta-\gamma) + \sum_{k=1}^{K}\left[X_{2k-1}\cos 2k\theta + X_{2k}\sin 2k\theta\right] \qquad (23)$$

where $\bar{h} = (C_r/\bar{C})h$ and $\bar{\varepsilon} = (C_r/\bar{C})\varepsilon$. The Fourier coefficients are mathematically determined to minimize a performance index. The performance index is chosen so that the designed bearings have excellent stability characteristics compared with conventional fluid-film bearings. Here, we consider a Jeffcott-rotor model to choose the performance index. The Jeffcott-rotor model contains a flat disk supported by a uniform, massless, flexible shaft, and the shaft is supported at the two ends by fluid-film bearings. The stability threshold speed P_{sf} for a Jeffcott rotor is written as

$$P_{sf}^2 = D\Big/\left\{\Omega_s^2[1 + D(\delta/C_r)]\right\} \qquad (24)$$

where

$$D = \left(c_{xx}k_{yy} + c_{yy}k_{xx} - c_{yx}k_{xy} - c_{xy}k_{yx}\right)\Big/\left(c_{xx} + c_{yy}\right) \qquad (25)$$

$$\Omega_s^2 = \left((D-k_{xx})(D-k_{yy}) - k_{xy}k_{yx}\right)\Big/\left(c_{xx}c_{yy} - c_{xy}c_{yx}\right), \qquad (26)$$

and δ is the static deflection of the rotor, which is induced by the gravity force applied to the disk, and Ω_s is called the whirl-frequency ratio. For the details of P_{sf}, see Child [1]. The whirl-frequency ratio is only dependent of the bearing coefficients and is completely independent of rotor mass and flexibility. In particular, if the rotor shaft is very flexible, that is, $\delta >> C_r$, the stability threshold speed is approximately simplified by

$$P_{sf}^2 \cong C_r\Big/\left(\Omega_s^2\delta\right) \qquad (27)$$

where C_r/δ is constant for the Jeffcott rotor and the stability threshold speed is inversely proportional to the whirl-frequency ratio. Therefore, a performance index is chosen to improve the stability characteristics of fluid-film bearings as follows:

$$J = \sum_{k=1}^{M} Max\left[\Omega_s^2(\bar{\varepsilon}_k), 0\right] \quad (0 < \bar{\varepsilon}_1 < \bar{\varepsilon}_2 < \cdots < \bar{\varepsilon}_M < 1) \qquad (28)$$

where if $A \geq B$, $Max[A, B] = A$, otherwise, $Max[A, B] = B$, and M is the number of eccentricity ratios. Note that the squared-values of the whirl frequency ratios could take a negative value as is suggested in Eq. (26); in this case the stability threshold speed does not exist, and the system cannot be destabilized for any rotating speed. The performance index is minimized subject to many constraints. The first M constraints are

$$\psi_k(\gamma_k, X) \equiv \left(\int_\Theta \tilde{p}_0(\bar{\varepsilon}_k, \gamma_k)\sin\theta d\theta \Big/ \int_\Theta \tilde{p}_0(\bar{\varepsilon}_k, \gamma_k)\cos\theta d\theta\right)^2 = 0$$

$$(k = 1,2,\cdots,M) \qquad (29)$$

Equation (29) defines γ_k as an attitude angle in a steady state, where it is assumed that the reaction force $\tilde{F}_0$ is directed along the negative Y axis (Fig. 1). In general, when the clearance magnitude is so large, fluid-film bearings have poor load capacity. Therefore, another constraint is necessary to limit the clearance magnitude to a favorable value as follows:

Table 1 Fixed values of some variables in the optimization

α	0.1
δ	$\pi/10$
$h_{\min}$	1.0×10^{-4}

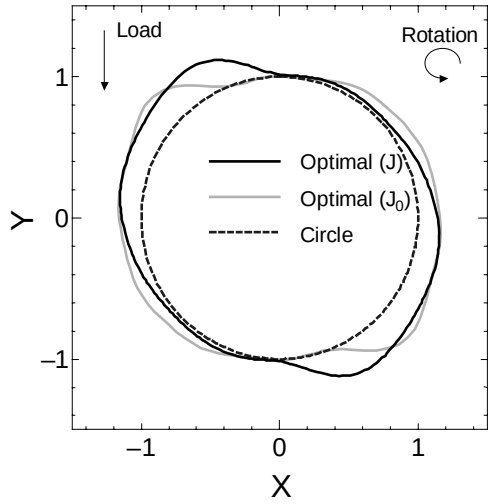

Fig. 3 Optimal clearance configuration of the designed bearings (α =0.1)

$$X^T X < \alpha^2 \tag{33}$$

where $X^T = [X_1 \quad X_2 \quad \cdots \quad X_{2K}]$, and α is a real number prescribed by a designer. The inequality constraint, Eq. (30), is converted into an equality constraint by introducing a dummy variable as follows:

$$\psi_{M+1}(X, d_1) = X^T X + d_1^2 - \alpha^2 = 0 \tag{31}$$

where d_1 is the dummy variable. Moreover, we have to introduce two constraints on the minimum value of the film thickness so that the film thickness takes a positive value at the largest eccentricity ratio, $\bar{\varepsilon} = \bar{\varepsilon}_M$. For this purpose, we need to find θ at which the film thickness takes the minimum value. It is now assumed that α is sufficiently small compared with unity. Equation (23) then suggests that the film thickness takes the minimum value close to $\theta = \pi + \gamma_M(\bar{\varepsilon}_M)$ when the eccentricity ratio is close to unity. Therefore, the film thickness is assumed to take the minimum value at $\theta = \pi + \gamma_M + \delta \sin q \equiv \theta_{\min}$, where δ is a small number. The sufficient condition to this assumption is given by

$$\psi_{M+2}(X, \gamma_M, q) = \frac{\partial \bar{h}}{\partial \theta}(\bar{\varepsilon}_M, \theta_{\min}) = 0 \tag{32}$$

Table 2 Optimal values of the Fourier coefficients

X_1	$-2.944268165383\times10^{-2}$
X_2	$8.851028532903\times10^{-2}$
X_3	$-1.918684997893\times10^{-2}$
X_4	$1.373155939494\times10^{-2}$
X_5	$-2.420024898786\times10^{-2}$
X_6	$1.210847806739\times10^{-3}$
X_7	$-1.009299723161\times10^{-2}$
X_8	$-6.115563402776\times10^{-3}$
X_9	$-2.316129747417\times10^{-3}$
X_{10}	$-2.443024926041\times10^{-3}$
X_{11}	$-2.615550427198\times10^{-4}$
X_{12}	$-2.139578080202\times10^{-3}$

Moreover, the film thickness has to take a positive value at $\theta = \theta_{\min}$ to give

$$\bar{h}(\bar{\varepsilon}_M, \theta_{\min}) \geq h_{\min} \tag{33}$$

where $h_{\min}$ is a positive and small number. Equation (33) is converted into an equality constraint in the same manner as Eq. (30):

$$\psi_{M+3}(X, \gamma_M, q, d_2) = \bar{h}(\bar{\varepsilon}_M, \theta_{\min}) - h_{\min} - d_2^2 = 0 \tag{34}$$

where d_2 is a dummy variable. The eccentricity ratio is again normalized by using the maximum value as

$$\bar{\varepsilon} = (1-\alpha)\varepsilon \tag{35}$$

where $\bar{\varepsilon}_M = 1-\alpha$ ($0 < \alpha < 1$), and ε naturally ranges from zero to unity. Moreover, the clearance configuration is then rewritten as

$$C = \frac{C_r}{1-\alpha}\left(1 + \sum_{k=1}^{K}\left[X_{2k-1}\cos 2k\theta + X_{2k}\sin 2k\theta\right]\right) \tag{36}$$

where the minimum clearance $C_r = \bar{C}(1-\alpha)$. Introducing $\Gamma = [\gamma_1 \quad \gamma_2 \quad \cdots \quad \gamma_M]^T$, the optimization problem leads to finding $\Pi = [X^T \quad \Gamma^T \quad d_1 \quad d_2 \quad q]^T$ to minimize the cost [Eq. (28)] subject to the constraints [Eqs. (29), (31), (32), and (34)], and is summarized as shown in Fig. 2. The present optimization problem differs from the previous one in the performance index subject to the same constraints. By the way, the authors previously solved another optimization problem for a clearance configuration of a fluid-film journal bearing, and the performance index was chosen as follows:

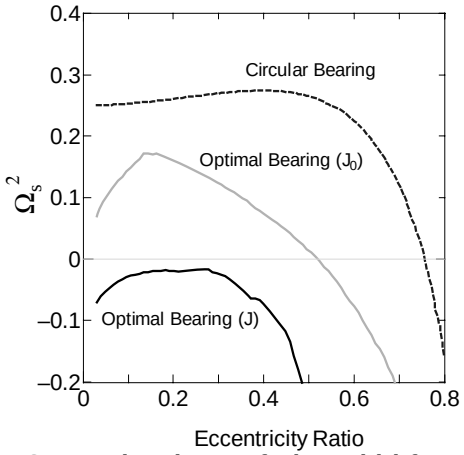

Fig. 4 Squared values of the whirl-frequency ratios for the designed bearings under the short-bearing assumption

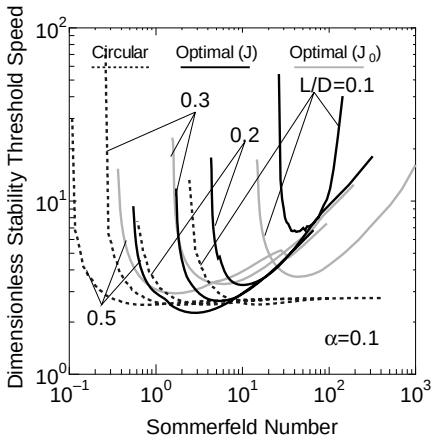

Fig. 5 Stability threshold speeds of a rigid rotor with the designed bearings for length-to-diameter ratios

$$J_0 = (1/2)\sum_{k=1}^{M} w_k \gamma_k^2 \; ; \quad \gamma_k = \gamma(\bar{\varepsilon}_k) \tag{37}$$

where w_k's weighting coefficients prescribed by a designer. This performance index is chosen because the attitude angle is reflected on magnitude of the cross coupling of the stiffness coefficients and because the whirl instability occurs due to the presence of skew-symmetric stiffness coefficients.

OPTIMIZATION RESULTS

The optimization problem is numerically solved when α, $h_{\min}$, and δ take the values shown in Table 1. The performance index is computed by sampling the whirl-frequency ratios at 20 eccentricity ratios that equidistantly range from 0.03 to 1.0 (M =20). The order of the Fourier series is unknown and initially set to one, and an optimization

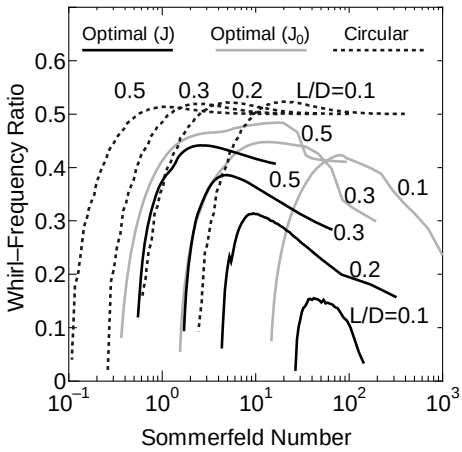

Fig. 6 Whirl-frequency ratios of the designed bearings for length-to-diameter ratios

problem is then solved in an iterative way, increasing the order incrementally by one. The value of the performance index evidently decreases as the order increases, and it finally converges to a value at which the order of the series takes the optimum value, K =6 in the present study. The optimal values of the Fourier coefficients are shown in Table 2. The optimal clearance configuration is compared with a full circle and the configuration previously designed with performance index J_0 as shown in Fig. 3. The two optimal configurations both resemble an offset two-lobe configuration [1], and, however, those three configurations are oriented in different directions to the applied load. It is also shown in Fig. 3 that the designed bearings have the same value of the minimum clearance, C_r, owing to Eqs. (32) and (34). Figure 4 shows squared values of the whirl-frequency ratios for the three configurations of fluid-film bearings. As is suggested in Eq. (26), Ω_s^2 could take a negative value, and the Jeffcott-rotor system cannot be destabilized at any frequency in this case. The designed bearing takes an imaginary value of the whirl-frequency ratio for all the eccentricity ratios as shown in Fig. 4, and, therefore, the whirl instability does not occur for the designed bearing. This conclusion is clearly limited to the case that the bearing length is infinitely short and could be deteriorated for fluid-film bearings with finite length. Equation (4) is numerically solved by a finite difference method to investigate stability characteristics of a finite-length bearing with the optimal configuration. Figure 5 shows the stability threshold speeds of a rigid-rotor system [1] for the designed bearings, which is computed by putting the static deflection $\delta = 0$ in Eq. (24). As is expected, the whirl instability occurs for a finite-length bearing, and, however, the instability region is limited to a narrow range of Sommerfeld number for D/L =0.1. Moreover, the whirl-frequency ratios are also computed as shown in Fig. 6. As is mentioned in the previous section, the whirl-frequency ratio is inversely proportional to the stability threshold speed of a Jeffcott rotor with a very flexible shaft. The whirl instability also occurs in the same range of Sommerfeld number as the rigid-rotor system. For $D/L = 0.1$, the dimensionless stiffness and damping coefficients of the designed bearing are shown in

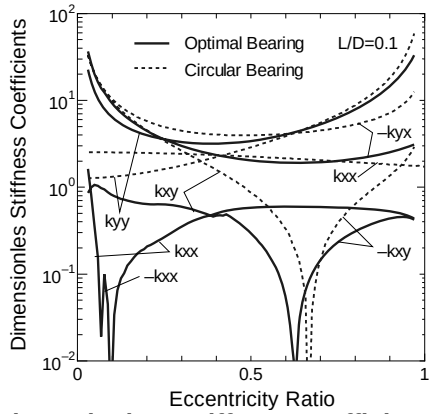

Fig. 7 Dimensionless stiffness coefficients for the optimal and circular bearings ($L/D = 0.1$)

Figs. 7 and 8, respectively. In contrast to the stiffness and damping coefficients of a full circular bearing, one of the direct

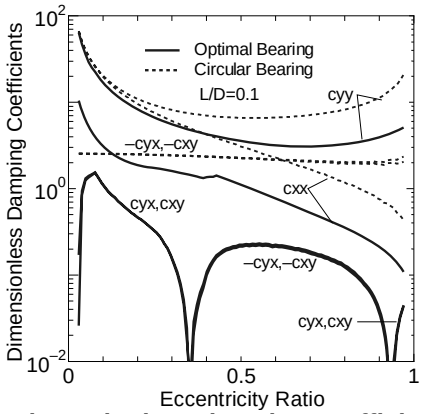

Fig. 8 Dimensionless damping coefficients for the optimal and circular bearings ($L/D = 0.1$)

stiffness terms, k_{xx} , takes a negative value at small eccentricity ratios, and the cross-coupled damping coefficients are positive for some eccentricity ratios. Furthermore, load capacity and friction torque of the designed bearing are computed and compared with those of a full circular bearing. Figures 9 and 10 show dimensionless force $\overline{F}_0$ and friction coefficients ς , respectively, for the optimal and circular bearings. It is shown in the two figures that the designed bearing has nearly the same magnitude of load capacity and friction torque as the full circular bearing. Figure 11 compares the attitude angles between the optimal and circular bearings. The optimal bearing causes the attitude angle steeply to decrease for higher Sommerfeld numbers, whereas the attitude angle monotonically increases as Sommerfeld number increase for the circular bearing. Figure 12 shows centerline pressure profiles for the optimal bearing at ε =0.2 and 0.5. The positive pressure is primarily developed at the lower part of the designed bearing. Figure 12 shows an effect of truncating the Fourier coefficients on the whirl-frequency ratios. The order of Fourier series is reduced from 6th to first by truncating higher terms incrementally by two. The whirl-frequency ratios of the designed bearing have no notable difference between K =5

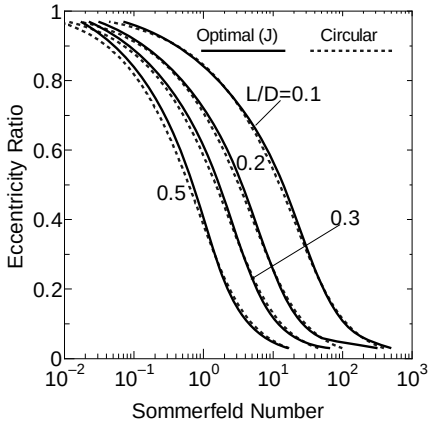

Fig. 9 Eccentricity ratios for the optimal and circular bearings

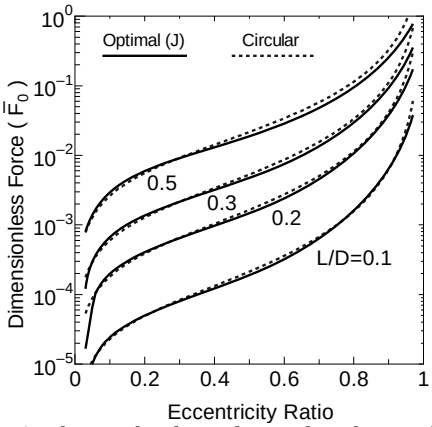

Fig. 10 Dimensionless force for the optimal and circular bearings

and 6, and are thus insensitive to the truncation. In other words, the machining tolerance for manufacturing the designed bearing does not need a significantly small value to keep the calculated values of the whirl-frequency ratio.

Swanson [14] found an optimal clearance configuration that minimizes the maximum value of the whirl-frequency ratios in a wide range of bearing loads at a specific rotating speed, whereas the designed bearing minimizes the squared sum of the whirl-frequency ratios from 0.03 to 1.0 of eccentricity ratios in dimensionless form. Swanson's clearance configuration [14] contains nonsymmetrical upper and lower lobes, and departs substantially from a full circle, and the sides are pinched in. This configuration is significantly different from the present one because the designed bearing is enforced by Eqs. (22) and (31) to have a rotationally symmetric configuration close to a full circle and no load capacity when the journal is situated at the bearing center in the present study. Moreover, Swanson's bearing (L/D =0.75) is free from the whirl instability over all the bearing loads at a specific rotation speed, whereas the designed bearing is not for finite-length cases in the present study.

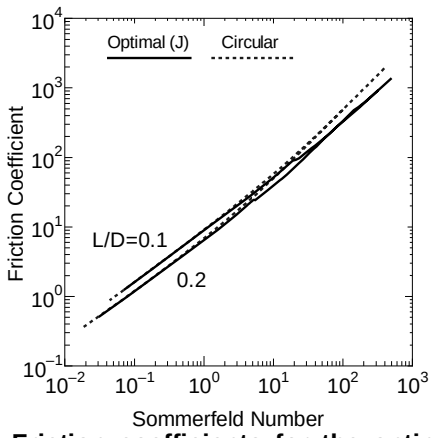

Fig. 11 Friction coefficients for the optimal and circular bearings

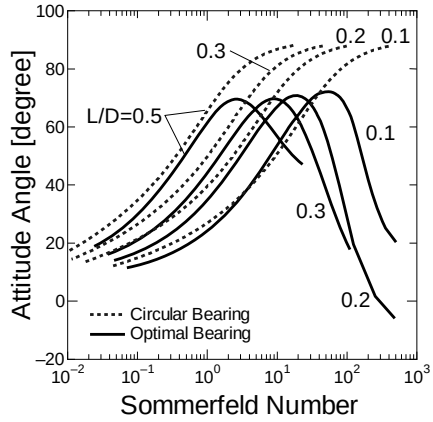

Fig. 12 Attitude angles for the optimal and circular bearings

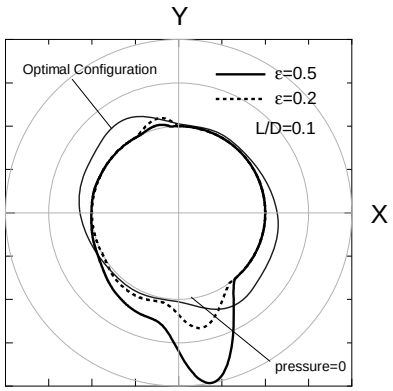

Fig. 13 Typical pressure distribution for the designed bearing

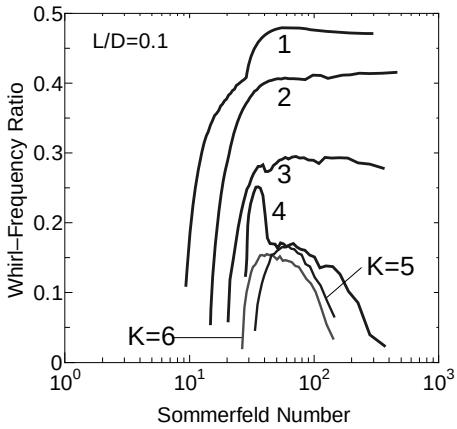

Fig. 14 Truncation effect of the optimal Fourier coefficients on the whirl-frequency ratios

CONCLUSIONS

A clearance configuration of fluid-film journal bearings is optimized to increase the stability threshold speed of a Jeffcott Rotor. The performance index is chosen as the sum of the whirl frequency ratios over a region of eccentricity ratio. The whirl-frequency ratios are inversely proportional to the stability threshold speeds of a very flexible Jeffcott rotor. It is shown that the designed bearing cannot destabilize the Jeffcott rotor for the short-bearing model. The stability threshold speeds are also computed for a fluid-film bearing with finite length. It is shown that the designed bearing significantly reduces the size of the unstable region for a small length-to-diameter ratio when compared with a full circular bearing.

ACKNOWLEDGMENTS

The authors would like to thank the anonymous reviewers for providing many valuable comments on this paper.

REFERENCES

1. Childs, D., 1993, *Turbomachinery Rotordynamics: Phenomena, Modeling*, and Analysis, John Willey & Sons, New York.
2. Lord Rayleigh, 1918,"Notes on the Theory of Lubrication," *Philosophical Magazine*, **35**, pp. 1-12.
3. Maday, C.J., 1970,"The Maximum Principle Approach to the Optimum One-Dimensional Journal Bearing," *ASME Journal of Lubrication Technology*, **92**, pp. 482-489.
4. Rohde, S.M., 1972," A Demonstrably Optimum One Dimensional Journal Bearing, " *ASME Journal of Lubrication Technology*, **94**, pp.188-192.
5. Rodhe, S.M., and McAllister, G.T., 1976," On the Optimization of Fluid Film Bearings," *Proceedings of the Royal Society of London*, **A351**, pp. 481-497.
6. Robert, M.P., 1990, "Optimization of Self-Acting Gas Bearings for Maximum Static Stiffness," *ASME Journal of Applied Mechanics*, **57**, pp. 758-761.
7. Robert, M.P., 1995," New Class of Sliders Numerically Designed for Maximum Stiffness," *ASME Journal of Tribology*, **117**, pp. 456-460.
8. Boedo, S., and Eshkabilov, S.L., 2003," Optimal Shape Design of Steadily Loaded Journal Bearings Using Genetic

Algorithms, "*STLE Tribology Transactions*, **46**, pp.134-143.
9. Hashimoto, H., 1997, "Optimum Design of High-Speed, Short Journal Bearings by Mathematical Programming, "*STLE Tribology Transaction*, **40**, pp. 283-293.
10. Wang, N.Z., Ho, C.L., and Cha, K.C., 2000," Engineering Optimum Design of Fluid-Film Lubricated Bearings, "*STLE Tribology Transactions*, **43**, pp. 377-386.
11. Matsuda, K., Kanemitsu, Y., and Kijimoto, S., 1998, " Optimal Geometry for Journal Bearings, " *Proceedings of 7th International Symposium on Transport Phenomena and Dynamics of Rotating Machinery*, **A**, ISROMAC-7, pp. 317-323.
12. Matsuda, K., Kanemitsu, Y., and Kijimoto, S., 2002," Fluid-Film Journal Bearings with Optimal Geometry, " *Proceedings of the ASME/STLE Joint International Tribology Conference 200*2, TRIB065.
13. Matsuda, K., Kanemitsu, Y., and Kijimoto, S., 2004, " Optimal Clearance Configuration of Fluid-Film Journal Bearings for Stability Improvement, " *ASME Journal of Tribology*, **126**, pp. 125-131.
14. Swanson, E., 2005, " Fixed-Geometry, Hydrodynamic Bearing Bearing with Enhanced Stability Characteristics," *STLE Tribology Transactions*, **48**, pp. 82-92.

